

Sulfonylureas exert antidiabetic action on adipocytes by inhibition of PPAR γ serine 273 phosphorylation



Bodo Haas^{1,*}, Moritz David Sebastian Hass^{1,2,6}, Alexander Voltz³, Matthias Vogel¹, Julia Walther¹, Arijit Biswas⁴, Daniela Hass^{3,5}, Alexander Pfeifer³

ABSTRACT

Objective: Sulfonylureas (SUs) are still among the mostly prescribed antidiabetic drugs with an established mode of action: release of insulin from pancreatic β -cells. In addition, effects of SUs on adipocytes by activation of the nuclear receptor peroxisome proliferator-activated receptor γ (PPAR γ) have been described, which might explain their insulin-sensitizing potential observed in patients. However, there is a discrepancy between the impact of SUs on antidiabetic action and their rather moderate *in vitro* effect on PPAR γ transcriptional activity. Recent studies have shown that some PPAR γ ligands can improve insulin sensitivity by blocking PPAR γ Ser-273 phosphorylation without having full agonist activity. It is unknown if SUs elicit their antidiabetic effects on adipocytes by inhibition of PPAR γ phosphorylation. Here, we investigated if binding of SUs to PPAR γ can interfere with PPAR γ Ser-273 phosphorylation and determined their antidiabetic actions *in vitro* in primary human white adipocytes and *in vivo* in high-fat diet (HFD) obese mice.

Methods: Primary human white preadipocytes were differentiated in the presence of glibenclamide, glimepiride and PPAR γ ligands rosiglitazone and SR1664 to compare PPAR γ Ser-273 phosphorylation, glucose uptake and adipokine expression. Transcriptional activity at PPAR γ was determined by luciferase assays, quantification of PPAR γ Ser-273 phosphorylation was determined by Western blotting and CDK5 kinase assays. *In silico* modelling was performed to gain insight into the binding characteristics of SUs to PPAR γ . HFD mice were administered SUs and rosiglitazone for 6 days. PPAR γ Ser-273 phosphorylation in white adipose tissue (WAT), body composition, glucose tolerance, adipocyte morphology and expression levels of genes involved in PPAR γ activity in WAT and brown adipose tissue (BAT) were evaluated.

Results: SUs inhibit phosphorylation of PPAR γ at Ser-273 in primary human white adipocytes and exhibit a positive antidiabetic expression profile, which is characterized by up regulation of insulin-sensitizing and down regulation of insulin resistance-inducing adipokines. We demonstrate that SUs directly bind to PPAR γ by *in silico* modelling and inhibit phosphorylation in kinase assays to a similar extend as rosiglitazone and SR1664. In HFD mice SUs reduce PPAR γ phosphorylation in WAT and have comparable effects on gene expression to rosiglitazone. In BAT SUs increase UCP1 expression and reduce lipid droplets sizes.

Conclusions: Our findings indicate that a part of SUs extra-pancreatic effects on adipocytes *in vitro* and *in vivo* is probably mediated via their interference with PPAR γ phosphorylation rather than via classical agonistic activity at clinical concentrations.

© 2024 The Author(s). Published by Elsevier GmbH. This is an open access article under the CC BY license (<http://creativecommons.org/licenses/by/4.0/>).

Keywords Sulfonylureas; PPAR γ ; White adipose tissue; Brown adipose tissue

1. INTRODUCTION

Type 2 diabetes mellitus (T2DM) has reached pandemic dimensions with estimated 537 million affected patients worldwide [1]. First-line therapy includes lifestyle modifications and dietary adjustments. Nevertheless, pharmacotherapeutic intervention is crucial to control long-term consequences of T2DM. A hallmark of T2DM is insulin resistance of multiple organs such as liver, muscle and adipose tissue.

Several antidiabetic medications are available which aim at correcting insulin resistance or to increase pancreatic insulin secretion [2]. Sulfonylureas (SUs) are a well-established class of antidiabetic drugs which are still extensively used and recommended for mono- or combination therapy in many parts of the world [3]. Their mode of action is stimulation of insulin secretion from pancreatic β -cells by binding to the sulfonylurea receptor 1 (SUR1) subunit of the adenosine triphosphate (ATP)-sensitive potassium channel on the plasma

¹Federal Institute for Drugs and Medical Devices (BfArM), Bonn, Germany ²Sonnen-Gesundheitszentrum - MVZ for Hemostaseology, Rheumatology, Endocrinology, General Medicine and Transfusion Medicine, Munich, Germany ³Institute of Pharmacology and Toxicology, University Hospital, University of Bonn, Bonn, Germany ⁴Institute of Experimental Hematology and Transfusion Medicine, University Hospital, University of Bonn, Bonn, Germany ⁵Institute for Diabetes and Cancer, Helmholtz Munich, German Center for Diabetes Research, Neuherberg, Germany

⁶ Bodo Haas and Moritz David Sebastian Hass contributed equally to this work.

*Corresponding author. Federal Institute for Drugs and Medical Devices (BfArM), Kurt-Georg-Kiesinger-Allee 3, 53175 Bonn, Germany. E-mail: bodo.haas@bfarm.de (B. Haas).

Received December 18, 2023 • Revision received March 4, 2024 • Accepted May 7, 2024 • Available online 10 May 2024

<https://doi.org/10.1016/j.molmet.2024.101956>

membrane [4]. Some pharmacodynamic effects of SUs such as improvement of insulin sensitivity or the ability to reduce circulating levels of pro-inflammatory cytokines while increasing levels of anti-inflammatory cytokines cannot be readily explained by increased insulin secretion [5–7]. It has previously been shown that SUs exert extra-pancreatic activity especially on white adipocytes. This includes induction of adipogenesis, increased glucose uptake and changes in adipokine expression profiles [8–13]. The proposed mechanism of action is activation of the nuclear receptor peroxisome proliferator-activated receptor γ (PPAR γ), a key regulator of adipocyte differentiation [14]. However, there is a discrepancy between the impact of SUs on antidiabetic action and their effect on PPAR γ transcriptional activity. While antidiabetic effects are already measurable at nanomolar to low micromolar concentrations in primary human adipocytes [10], an increase of PPAR γ promoter activity occurs in the higher micromolar range in *in vitro* experiments [8,12,13,15] and thus leaves the question whether all effects are indeed mediated by transcriptional activation of PPAR γ at clinically relevant concentrations. PPAR γ can be activated by endogenous ligands such as fatty acids and their metabolites, as well as by thiazolidinediones (TZDs) [16,17]. TZDs directly bind to the ligand-binding domain (LBD) of PPAR γ , thereby activating the transcription of target genes, which are involved in many metabolic pathways. Due to their insulin-sensitizing effect, TZDs have been used to treat metabolic disorders such as T2DM, however the clinical use has subsequently declined in the last years owed to adverse effects [18]. Binding of ligands to PPAR γ not only activates transcription but also blocks cyclin-dependent kinase 5 (CDK5) and/or extracellular signal-regulated kinase (ERK)-mediated phosphorylation of PPAR γ at serine 273 (Ser-273). Phosphorylation of PPAR γ by CDK5/ERK does not alter its adipogenic activity, but modifies expression of a specific set of genes with impact in obesity and diabetes [19–21]. Classical transcriptional activation of PPAR γ , which mediates at least some of the undesirable side effects of chronic PPAR γ activation, appears to be independent from Ser-273 phosphorylation. The exact mechanism is still not fully clear but it is suggested that selective co-regulator recruitment to PPAR γ is regulated in a phosphorylation-dependent manner and controls expression of diabetes-related genes [22,23]. Prevention of PPAR γ Ser-273 phosphorylation in adipose tissues and skeletal muscle protects mice from insulin resistance. This is associated with decreased levels of growth differentiation factor 3 (GDF3), which is a member of the transforming growth factor β (TGF- β) superfamily that reduces insulin sensitivity by inhibition of bone morphogenic protein (BMP) signaling [24]. In addition, the protein phosphatase Mg²⁺/Mn²⁺-dependent 1A (PPM1A), which dephosphorylates Ser-273 of PPAR γ can restore dysregulated genes involved in diabetes progression in obese mice [25]. Thus, PPAR γ agonism is not necessarily correlated with antidiabetic action. Interestingly, PPAR γ ligands which exert only low agonistic activity, like the experimental substance SR1664, are able to block PPAR γ phosphorylation at Ser-273 and still have antidiabetic activity without inducing adverse effects such as fluid retention, bone fractures and weight gain in mice [20,26,27]. The inhibition of PPAR γ phosphorylation requires binding of ligands to the PPAR γ LBD, resulting in conformational changes that interfere with the ability of CDK5/ERK to phosphorylate Ser-273 [20]. Most of these experiments were performed with murine cells and so far data from primary human white adipocytes are lacking. In addition, it has been proposed that SUs bind to the PPAR γ LBD [8,12,13,15] but their impact on PPAR γ phosphorylation remains elusive. In this study, we investigated the binding characteristics of the widely prescribed SUs glibenclamide and glimepiride, representative of a

conventional (old) and a modern SU, respectively, to PPAR γ focusing on the question whether SUs inhibit PPAR γ Ser-273 phosphorylation in comparison to the PPAR γ ligands rosiglitazone and SR1664. We found that SUs interfere with PPAR γ Ser-273 phosphorylation in the nanomolar range. Despite their low PPAR γ transcriptional activity, SUs still elicited an antidiabetic impact on primary human white adipocytes comparable to SR1664. In high-fat diet (HFD) obese mice short-term SU treatment reduced PPAR γ Ser-273 phosphorylation in white adipose tissue (WAT) resulting in increased adipogene expression and mRNA reduction of the adipose tissue macrophage marker *F4/80*. In brown adipose tissue (BAT), SUs induced uncoupling protein 1 (UCP1) expression to a similar extent as rosiglitazone but without increasing adipogenesis and BAT weight. Our findings indicate that extra-pancreatic effects frequently observed in patients treated with SUs are probably at least in part driven by inhibition of PPAR γ Ser-273 phosphorylation in adipocytes rather than via classical PPAR γ agonistic activity.

2. MATERIAL AND METHODS

2.1. Animals

8-week-old male C57Bl/6N mice were fed a HFD (60% energy from fat; Ssniff HFD: EF D12492, #E15741–347) for 16 weeks. Mice were maintained at the Haus für experimentelle Therapie, University Hospital Bonn, or at the Institute of Pharmacology and Toxicology, University Hospital Bonn, during experiments on a daily cycle of 12 h light (06:00 to 18:00) and 12 h darkness (18:00 to 06:00), at 23 ± 1 °C, and were allowed free access to chow and water. Health status was checked frequently and included determination of body weight, observation of unprovoked behavior and responses to external stimuli, as well as assessment of physical appearance. HFD mice were injected intraperitoneally (i.p.) twice daily with 10 mg/kg glimepiride, glibenclamide, rosiglitazone (all Sigma–Aldrich) dissolved in EtOH 10%, PEG 40%, H₂O 50% or vehicle alone for 6 days. Studies including pharmacokinetics were performed 1 h after the last dose or after overnight starving. All animal experiments have been approved by the local authority Landesamt für Natur, Umwelt und Verbraucherschutz, NRW, Germany (reference: 84–02.04.2014.A202).

2.2. Body composition analysis

Body composition was analyzed using a table Bruker Minispec LF50H [28].

2.3. Glucose tolerance test

After the last drug treatment animals were fasted overnight. Eight μ l/g body weight of glucose solution (2.5 g/mL) were injected i.p. and glucose was measured at indicated time points post injection. Tail vein was punctured and blood was analyzed with an Accu-Chek Aviva Nano analyzer and dipsticks (Roche).

2.4. Serum analysis

Serum was collected by blood centrifugation (2000 g, 10 min at RT) and frozen.

For adiponectin determination, serum was diluted 1:30000 in ELISA buffer and adiponectin concentrations were determined using the Adiponectin Mouse ELISA Kit (Invitrogen) according to the manufacturer's instructions.

To determine serum lipids the Piccolo Lipid Plus Panel was used (ABAXIS Europe GmbH) in conjunction with a Piccolo Xpress analyzing system according to the manufacturer's instructions.

2.5. Pharmacokinetic analysis

Serum concentrations of glibenclamide, glimepiride and rosiglitazone were analyzed by liquid chromatography – tandem mass spectrometry. All samples were fortified with 10 ng/mL tolbutamide (Sigma–Aldrich) as internal standard. Respective volumes of mouse serum were precipitated with the threefold volume of acetonitrile ($-20\text{ }^{\circ}\text{C}$) and centrifuged for 10 min at 14,000 g. The supernatant was dried under vacuum conditions at $60\text{ }^{\circ}\text{C}$ and subsequently reconstituted with 0.2% formic acid. For all measurements a QTRAP 6500 triple quadrupole MS (Sciex) coupled to a Nexera UPLC (Shimadzu) was used under positive electrospray ionization (ESI) conditions. The system was equipped with an Accucore C8 ($50 \times 3\text{ mm}$, $2.6\text{ }\mu\text{m}$ particle size, Thermo Fisher). Gradient elution was applied over 14 min by using (A) 0.2% formic acid, pH 2.5 and (B) acetonitrile with T_{min}/B [%] 0.2/2, 8.0/60, 10.0/100, 12.0/100, 12.1/2, and 14.0/2. For quantification (+) MRM ion transitions were m/z 494.1 to 169.0, 491.2 to 126.1, 358.1 to 135.1 for glibenclamide, glimepiride and rosiglitazone, respectively. Collision energies (CE) were set to 35 [eV]. Tolbutamide was determined with m/z 271.1 to 155.1 and a CE with 27 [eV].

2.6. Immunohistochemistry

Five-micrometer paraffin-embedded gonadal WAT (gWAT) and interscapular BAT (iBAT) sections were hydrated and blocked with 2.5% normal goat serum–PBST (phosphate-buffered saline, 0.1 % Tween-20) for 1 h at room temperature. Primary antibodies (GLUT4, 1:50, Santa Cruz; F4/80, 1:10, Invitrogen; UCP1, 1:500, custom made) were applied overnight at $4\text{ }^{\circ}\text{C}$. After washing three times with PBST, secondary antibody against rabbit (SignalStain Boost IHC, Cell Signaling) was applied for 1 h at room temperature and developed with the DAB Kit (Vector Laboratories) according to the manufacturer's instructions. WAT sections were counterstained with hematoxylin before dehydration. Standard hematoxylin and eosin (H&E) staining was performed with BAT sections. Sections were mounted with RotiHistokit (Carl Roth). Quantification of lipid droplet sizes in H&E-stained BAT sections was analyzed and calculated using the Adiposoft plugin for Fiji (ImageJ). Large lipid droplets were defined as surface $>300\text{ }\mu\text{m}^2$. One 20x magnification frame of BAT per mouse was scored.

2.7. Differentiation of primary human preadipocytes and murine 3T3-L1 preadipocytes

Human primary preadipocytes prepared from liposuction material were obtained from PromoCell and differentiated as previously described [10]. In brief, cells were expanded in growth medium (PromoCell) and differentiation (day 0) was initiated by switching for three days to differentiation medium (PromoCell). Thereafter, the cells were cultured in nutrition medium (PromoCell) containing glibenclamide, glimepiride, rosiglitazone or SR1664 (all Sigma–Aldrich) dissolved in DMSO until day 21 if not otherwise stated. 3T3-L1 preadipocytes were obtained from the American Type Culture Collection (ATCC) and were cultured in Dulbecco's modified Eagle's medium (DMEM, Invitrogen) and 10% fetal bovine serum. Differentiation was induced as previously reported [29]. Glibenclamide, glimepiride, rosiglitazone or SR1664 were added to culture media from induction of differentiation on (day 0) until day 7 if not otherwise stated. Human (Sigma–Aldrich) or murine (Miltenyi Biotec) tumor necrosis factor α (TNF α) were dissolved in water and added to culture media as indicated.

2.8. Oil Red O staining and triglyceride measurement

Lipid accumulation of differentiated adipocytes was determined by Oil red O staining or enzymatic determination of triglyceride content. For

Oil red O staining, cells were washed in PBS and fixed with 4 % paraformaldehyde at $4\text{ }^{\circ}\text{C}$ for 1 h. Thereafter 1 mL Oil Red O solution (1.25 mg/mL) was added to the wells and incubated for 1 h at room temperature. Finally, cells were washed three times with aqua dest. and were evaluated by light microscopy.

For determination of the triglyceride content, cells were washed once with PBS and after addition of TX lysis buffer (150 mM NaCl, 0.05% Triton X-100, 10 mM Tris–HCl pH 8), wells were immediately frozen at $-80\text{ }^{\circ}\text{C}$. Cells were thawed on ice, sonicated and resuspended. Triglyceride reagent (Sigma–Aldrich) was added and after incubation for 3 h at room temperature in the dark, absorption at 540 nm was measured against TX lysis buffer and a triglyceride standard. Triglyceride content was normalized to the protein content of the sample.

2.9. Western blotting

Proteins from cells and gWAT were extracted with RIPA lysis buffer (150 mM NaCl, 50 mM Tris–HCl pH 7.5, 1% Nonidet P40, 0.25% Na-deoxycholat, 0.1% SDS) containing Complete Protease Inhibitor Cocktail (Roche), 1 mM Na_3VO_4 , and 10 mM NaF. The protein content was determined with the BCA method. Western blotting was performed as previously described [30] using the following primary antibodies: anti-aP2 (1:1000), anti-PPAR γ (1:1000), anti-H1 (1:1000), anti- β -actin–HRP (1:20000; all Santa Cruz Biotechnology), anti-CDK substrate antibody (1:500) to detect phospho-Ser in the consensus motif for CDK substrate proteins (KSPXK) and anti-CDK5 (1:1000; all Cell Signaling Technology). A rabbit polyclonal phospho-specific antibody against human PPAR γ 2 Ser-273 was custom made by Thermo Fisher Scientific with a synthetic phospho-peptide corresponding to residues surrounding Ser-273 of PPAR γ 2 (Ac-KTTDKpSPFVIYD-C) coupled to KLH.

2.10. RNA extraction and quantitative Real-time-PCR

RNA from cells, gWAT and iBAT were extracted with Trizol (Invitrogen). Reverse transcription was performed using the Transcriptor First Strand cDNA Synthesis Kit (Roche). Quantitative Real-time PCR (qRT-PCR) was performed with SYBR Green (Roche) using a HT7900 instrument (Applied Biosystems). Relative mRNA expression was determined by the $\Delta\Delta$ –Ct method normalized to human glyceraldehyde 3-phosphate dehydrogenase (*GAPDH*) or murine hypoxanthine guanine phosphoribosyl transferase (*Hprt*). Primer pairs are presented in Table S1.

2.11. In vitro CDK5/P35 kinase assay

In vitro CDK5/P35 kinase assays were performed according to the manufacturer's instructions (Cell Signaling Technology). $0.5\text{ }\mu\text{g}$ of recombinant PPAR γ LBD (Cayman Chemicals) or purified histone H1 protein (New England Biolabs) and active CDK5/P35 kinase (Millipore) dissolved in kinase assay buffer were pre-incubated with different concentrations of the compounds for 30 min at room temperature as indicated. Kinase reaction was started by adding ATP to a final concentration of $200\text{ }\mu\text{M}$ for 15 min at $30\text{ }^{\circ}\text{C}$.

For Western blotting kinase reactions were stopped by the addition of Laemmli buffer and heating for 5 min at $99\text{ }^{\circ}\text{C}$. Ten μL of the reaction were subjected to Western blotting (see above).

To quantitatively measure kinase activity the amount of adenosine diphosphate (ADP) produced during the kinase reaction was determined with the ADP-Glo kinase assay (Promega). Kinase reaction was stopped and the ADP content determined in a 96-well format according to the manufacturer's instructions. Luminescence was measured with an EnSpire Plate Reader (Perkin Elmer).

2.12. Glucose uptake assay

Glucose content in culture media was determined with the Glucose Colorimetric Assay Kit (Cayman Chemicals) according to the manufacturer's protocol. Total glucose uptake was calculated by subtracting obtained glucose concentrations of supernatants of treated cells from glucose content of native culture medium.

2.13. *In silico* modelling

In silico analysis (i.e., ligand docking and structural alignment/comparison) was performed with pre-determined ligand bound crystal structures as well as modelled structures of PPAR γ . The details of the methods used are presented in [Supplementary Materials](#).

2.14. Luciferase assay

Luciferase assays were performed according to a published protocol using the Dual-Luciferase Reporter Assay System (Promega) [31]. In brief, HEK-293T cells were transfected using Lipofectamine 2000 (Invitrogen) with plasmids containing PPAR γ 2 (pBabe bleo human PPAR γ 2), RXR α (pSV Sport RXR α), PPRE (DR1X3) firefly luciferase reporter (PPRE X3-TK-luc) and renilla luciferase (pRL-TK-Renilla, Promega). PPRE X3-TK-luc (Addgene plasmid #1015) and pSV Sport RXR α (Addgene plasmid #8882) were a kind gift from Bruce Spiegelman [32,33]. pBabe bleo human PPAR γ 2 (Addgene plasmid #11439) was a kind gift from Ronald Kahn. Following an overnight transfection, cells were treated with compounds as indicated for 24 h.

2.15. Statistical analysis

Concentration effect curves were fitted to data points by nonlinear regression analysis using the four-parameter logistic equation using Prism software (GraphPad). Statistical significance was determined using one-way or two-way ANOVA analysis of variance with Dunnett's or Tukey's post-hoc tests to compare differences among multiple groups as indicated.

3. RESULTS

3.1. Transcriptional activity, induction of adipogenesis and suppression of cytokine expression by SUs, rosiglitazone and SR1664 in primary human white adipocytes

TZDs such as rosiglitazone are classical PPAR γ full agonists and increase expression of adipogenic genes in adipocytes, which rely on both, PPAR γ transcriptional activity and PPAR γ Ser-273 phosphorylation. Instead, compounds like the PPAR γ ligand SR1664 display low PPAR γ transcriptional activity but block phosphorylation of PPAR γ at Ser-273 thereby modulating transcription of a subset of genes [19,20]. PPAR γ as a transcription factor binds to the PPAR response element (PPRE) in the promoters of its target genes to activate expression. In order to directly compare the PPAR γ transcriptional activity of SUs to rosiglitazone and SR1664, we performed luciferase reporter assays. Therefore, we transfected HEK293T cells with PPAR γ and a PPRE luciferase reporter construct in the presence of different concentrations of the compounds. Both SUs and SR1664 only weakly increased the reporter activity (1.8-, 2.2-, 3.3-fold at 10 μ M for SR1664, glimepiride and glibenclamide, respectively) as compared to rosiglitazone (8-fold increase at 10 μ M; [Figure 1A](#)). We used primary human preadipocytes as a model system to investigate if SUs, despite low PPAR γ transcriptional activity, still can have an impact on adipogenesis when applied during differentiation. Glibenclamide significantly increased adipogenesis almost as strong as rosiglitazone as determined by Oil Red O staining and triglyceride quantification. A statistically significant but lower increase in lipid accumulation was observed for glimepiride and SR1664

([Figure 1B](#)). This is in contrast to murine white adipocytes where SR1664 did not induce adipogenesis [20,27]. Expression of adipogenic markers was determined by qRT-PCR and Western blotting. Adiponectin, *aP2* and *CD36* mRNA expression was significantly increased by glibenclamide and rosiglitazone. Instead, glimepiride and SR1664 only increased *aP2* and adiponectin mRNA expression, while *CD36* was not affected ([Figure 1C](#)). The increase of adiponectin expression after SU treatment is of particular interest as it depends on PPAR γ Ser-273 phosphorylation [19,20]. Leptin mRNA was only significantly increased after rosiglitazone treatment showing that strong PPAR γ agonist activity is required for its expression in human adipocytes ([Figure 1C](#)). In line with the observed lipid accumulation, *aP2* protein expression was significantly increased 10- and 12-fold by glimepiride and glibenclamide, respectively, as compared to 20-fold by rosiglitazone ([Figure 1D](#)). Although SR1664 affected *aP2* protein expression, this increase was not significantly different from the control (4-fold) ([Figure 1D](#)). These data show that transcriptional activation of PPAR γ by glibenclamide is still sufficient to enhance adipogenic differentiation of primary human white preadipocytes in a similar fashion to rosiglitazone when applied at equimolar concentrations. In line with the weaker PPAR γ transcriptional activity ([Figure 1A](#)), adipogenic potency of glimepiride was lower as compared to rosiglitazone and glibenclamide.

Obesity and T2DM are characterized by increased levels of pro-inflammatory cytokines and free fatty acids circulating in blood and tissues [34]. TZDs and SUs are able to reduce expression of pro-inflammatory cytokines in human adipocytes [10]. To directly compare the effect of the four compounds on cytokine expression during differentiation, we also performed qRT-PCR analyses. SUs and rosiglitazone suppressed expression of all cytokines tested ([Figure 1E](#)). In contrast, SR1664 only diminished mRNA expression of members of the C-X-C motif chemokine ligand (*CXCL*) family but did not significantly affect interleukin 6 (*IL6*) and monocyte chemoattractant protein 1 (*MCP1*) expression ([Figure 1E](#)). Thus, modulation of expression of *IL6* and *MCP1* does not seem to depend on PPAR γ Ser-273 phosphorylation in primary human white adipocytes.

3.2. SUs block PPAR γ Ser-273 phosphorylation and counteract TNF α -induced antidiabetic effects *in vitro* in white adipocytes

TNF α induces phosphorylation of PPAR γ at Ser-273 in murine adipocytes subsequently promoting insulin resistance [19,20]. To test if TNF α was able to induce insulin resistance in our cellular system and if this can be reverted by SUs as compared to rosiglitazone and SR1664, we measured overall glucose uptake and glucose transporter 4 (*GLUT4*) mRNA expression of primary human white adipocytes after stimulation with TNF α . Preincubation of cells with rosiglitazone completely prevented TNF α -induced reduction of glucose uptake ([Figure 2A](#)) and diminished suppression of *GLUT4* mRNA expression ([Figure 2B](#)). But, also SUs and SR1664 counteracted the TNF α -induced effects ([Figure 2A,B](#)). This shows that glucose trafficking during TNF α -induced diabetic processes in human adipocytes predominantly relies on PPAR γ Ser-273 phosphorylation and not on PPAR γ agonist activity.

Next, we analyzed the underlying mechanisms in both murine and human white adipocytes. TNF α induced PPAR γ Ser-273 phosphorylation in primary human white adipocytes in a concentration-dependent manner as shown by phospho-PPAR γ Ser-273 Western blots ([Figure S1A](#)). To address if SUs block PPAR γ Ser-273 phosphorylation, we pre-incubated primary human white adipocytes with rosiglitazone, SR1664 and SUs prior to stimulation with TNF α . Treatment with all compounds resulted in a significant reduction in TNF α -induced PPAR γ phosphorylation, bringing phospho-Ser-273

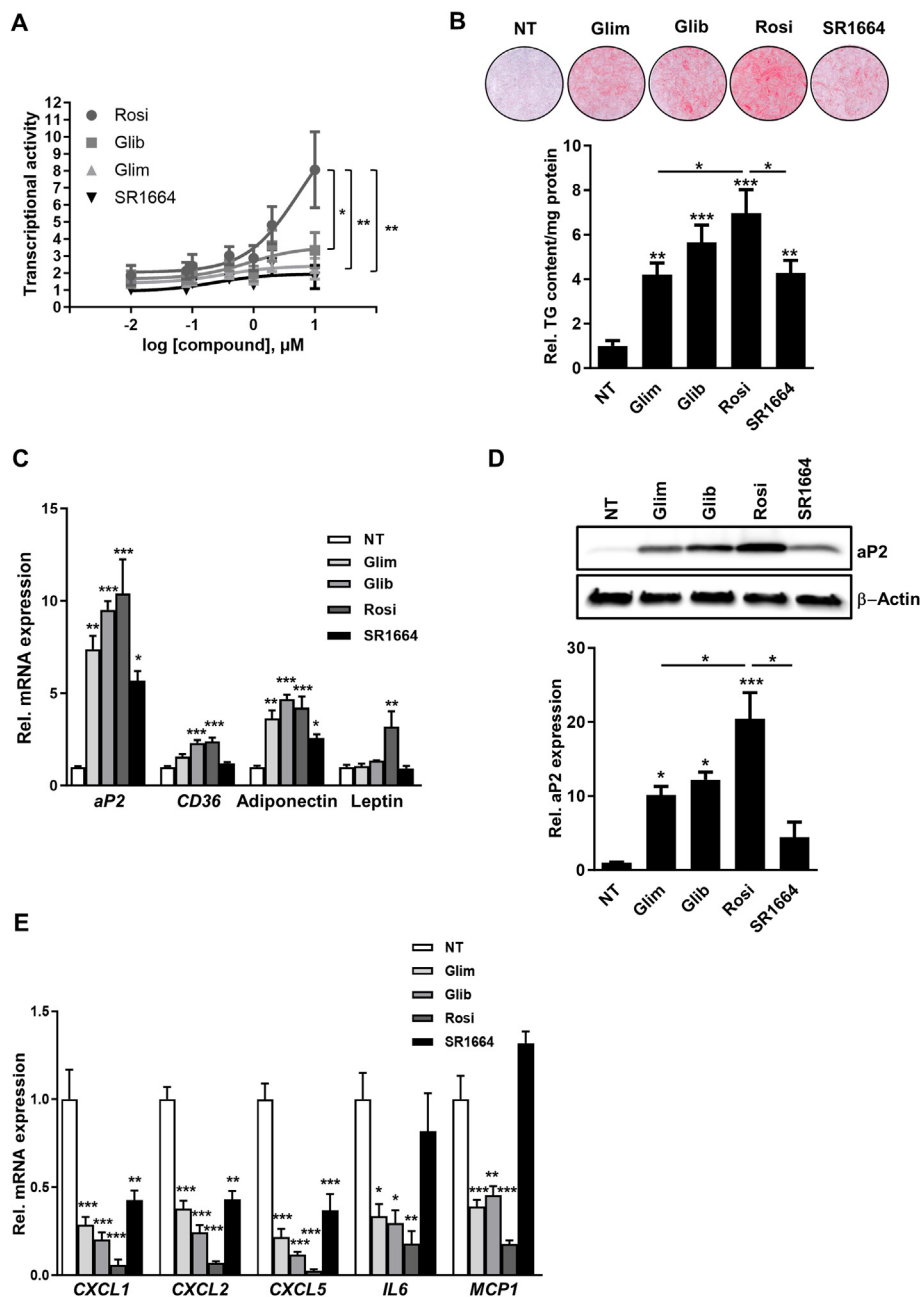


Figure 1: Transcriptional activity of sulfonylureas, rosiglitazone and SR1664, and effects on primary human white preadipocytes during differentiation.

(A) Transcriptional activity (luciferase assays) of a PPAR response element (PPRE) in HEK293T cells following treatment with increasing concentrations (0.01–10 μM) of glimepiride (Glim), glibenclamide (Glib), rosiglitazone (Rosi) and SR1664 ($n = 4$). Primary human white preadipocytes were differentiated in the presence of 2.5 μM Glim, Glib, Rosi and SR1664 until Day 21. (B) Red O staining of differentiated adipocytes (upper panel). Triglyceride (TG) content was quantified using an enzymatic assay and normalized to the protein content of the sample (lower graph, $n = 4$). (C) mRNA expression of adipogenic markers *aP2*, adiponectin, *CD36* and leptin was determined by qRT-PCR ($n = 5$). (D) *aP2* protein expression was assessed by Western blotting. β -Actin Western blot was performed to control for loading (upper panels). Quantification of relative *aP2* expression vs. β -Actin ($n = 3$, lower graph) (E) mRNA expression of pro-inflammatory cytokines *CXCL1*, *CXCL2*, *CXCL5*, *IL6* and *MCP1* was determined by qRT-PCR ($n = 5$). Data are represented as means \pm SEM. *, $p \leq 0.05$; **, $p \leq 0.01$; ***, $p \leq 0.001$ vs NT or as indicated, One-way ANOVA with Dunnett's or Tukey's post-hoc test. NT, not treated.

levels close to baseline (Figure 2C). A similar effect of SUs was also observed in differentiated murine 3T3-L1 adipocytes (Figure S1B). To exclude indirect effects of SUs on CDK5 kinase activity, we assessed whether SUs modulate PPAR γ Ser-273 phosphorylation using a CDK5 kinase assay. SUs reduced phosphorylation of the PPAR γ LBD as shown

with a CDK5 substrate specific antibody similar to rosiglitazone and SR1664 (Figure 2D). It is noteworthy that this inhibition is not caused by a general inhibition of CDK5 activity, as incubation with the test compounds did not inhibit the ability of CDK5 to phosphorylate its well-known substrate histone H1 (Figure 2E).

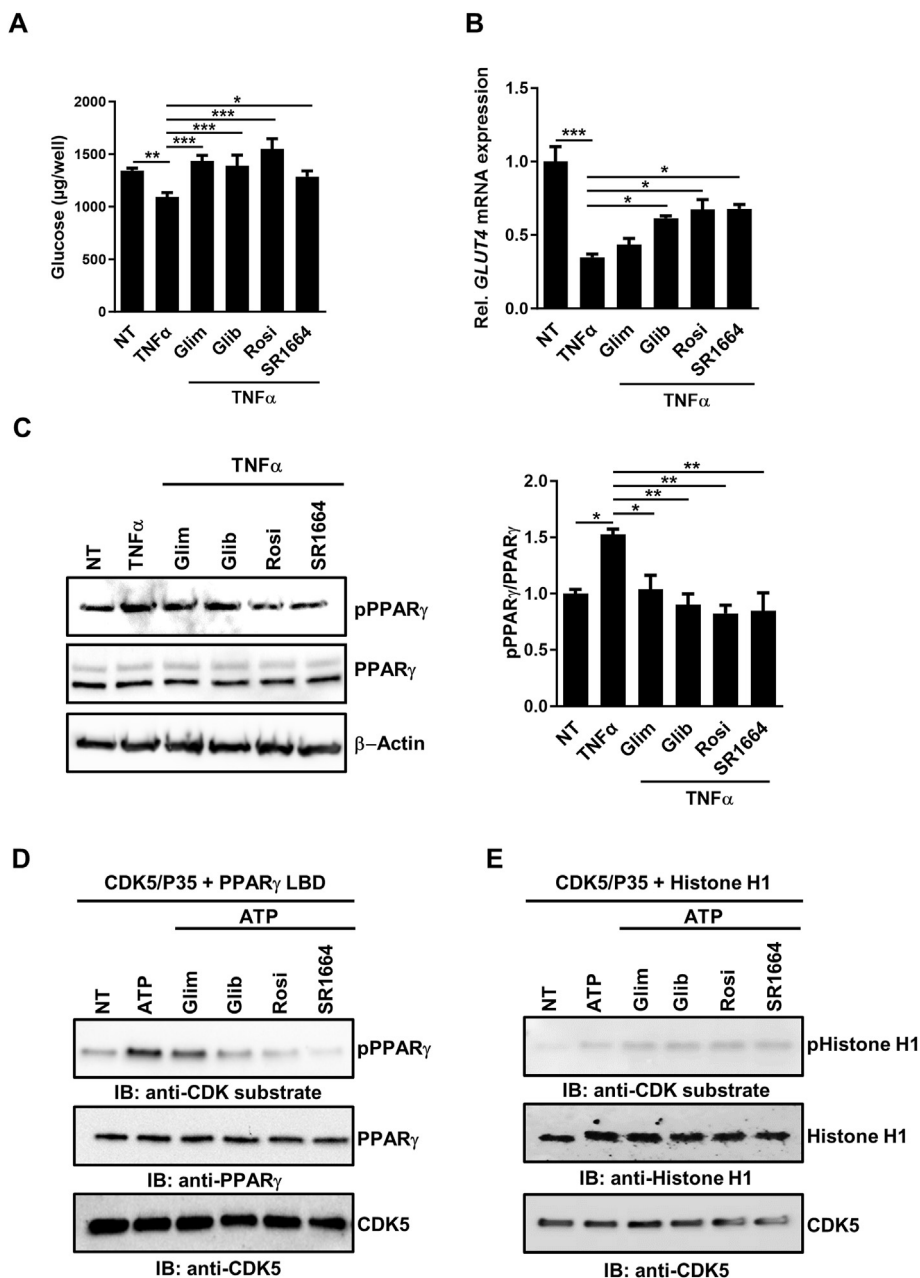


Figure 2: Sulfonylureas, rosiglitazone and SR1664 have antidiabetic effects and block PPAR γ Ser-273 phosphorylation *in vitro*.

(A) Total glucose uptake ($n = 6$) and (B) *GLUT4* mRNA expression ($n = 3$) of differentiated primary human white adipocytes pre-incubated with 2.5 μM glimepiride (Glim), glibenclamide (Glib), rosiglitazone (Rosi) and SR1664 for 45 min prior to treatment with 5 ng/mL human TNF α for 48 h. (C) Western blot against phosphorylated PPAR γ at Ser-273 (pPPAR γ) of differentiated primary human white adipocytes pre-treated with 2.5 μM Glim, Glib, Rosi and SR1664 for 45 min prior to treatment with 5 ng/mL human TNF α for 60 min. PPAR γ and β -Actin Western blots were performed to control for loading (left panels). Quantification of relative PPAR γ phosphorylation vs. PPAR γ expression is shown in the right graph ($n = 4$). (D) *In vitro* CDK5 kinase assay on PPAR γ LBD incubated with 2.5 μM Glim, Glib, Rosi and SR1664. Kinase assays were subjected to Western blotting with a CDK substrate specific antibody, PPAR γ or CDK5. (E) *In vitro* CDK5 kinase assay on Histone H1 incubated with 2.5 μM Glim, Glib, Rosi and SR1664. Kinase assays were subjected to Western blotting with a CDK substrate specific antibody, Histone H1 or CDK5. Data are represented as means \pm SEM. *, $p \leq 0.05$; **, $p \leq 0.01$; ***, $p \leq 0.001$ vs TNF α , One-way ANOVA with Dunnett's post-hoc test. IB, immunoblot; NT, not treated.

3.3. Concentration-response relationships of PPAR γ Ser-273 phosphorylation

To further study the SU-induced effects, we recorded concentration-response relationships of CDK5 kinase inhibition and determined half-maximal inhibitory concentrations ($\text{IC}_{50\text{s}}$). To this end, we quantitatively measured the amount of ADP produced during the

kinase reaction by a luminescent ADP detection assay. Notably, glibenclamide showed a comparable phosphorylation inhibition of the PPAR γ LBD to rosiglitazone and SR1664 with $\text{IC}_{50\text{s}}$ of 25 nM, 21 nM and 17 nM, respectively (Figure 3A–C) while glimepiride displayed an approximately 15-fold lower potency (IC_{50} : 378 nM; Figure 3D).

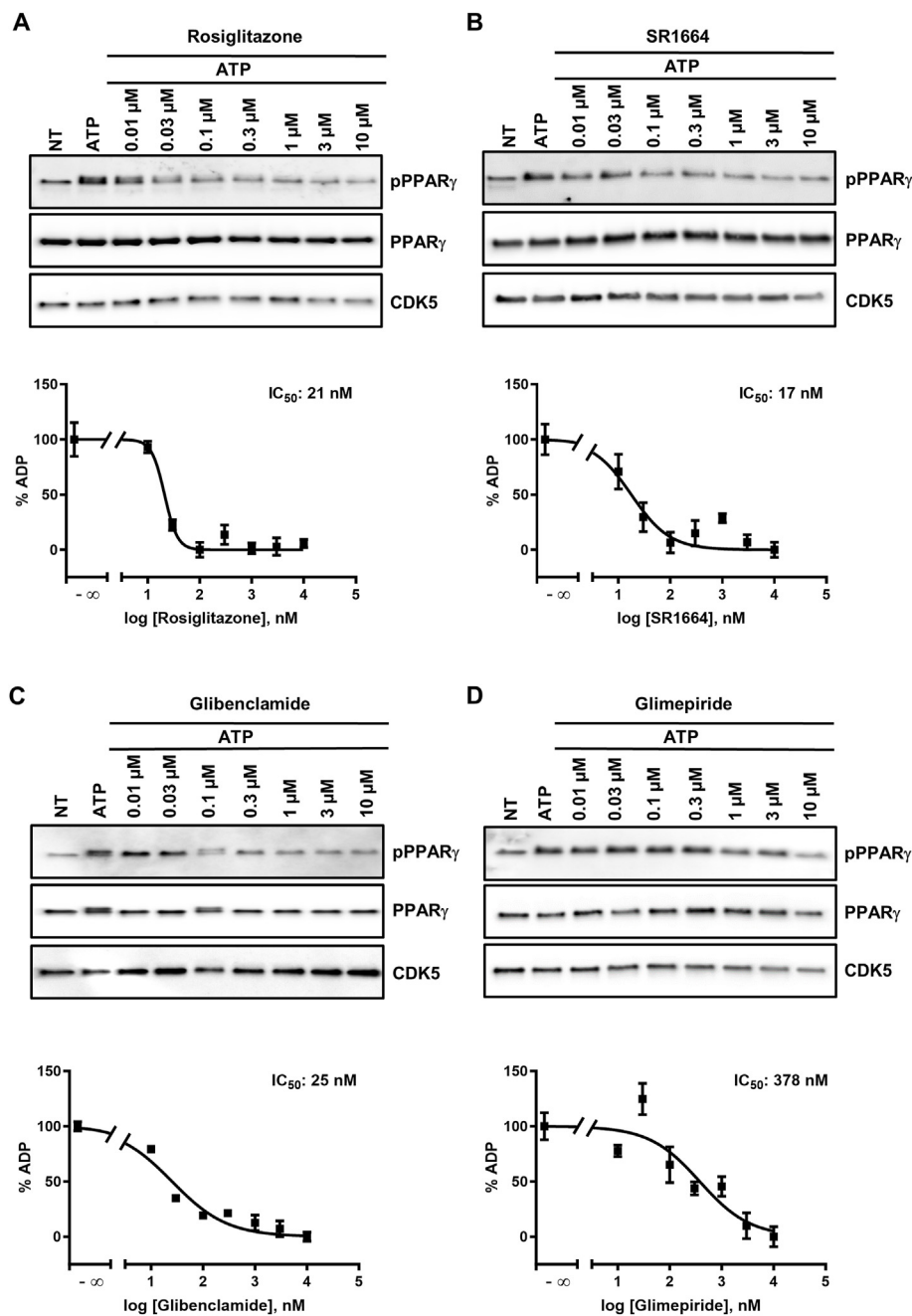


Figure 3: Sulfonylureas inhibit PPAR γ Ser-273 phosphorylation in a concentration-dependent manner *in vitro*.

In vitro CDK5 kinase assays on PPAR γ LBD incubated with increasing concentrations (0.01–10 μ M) of (A) rosiglitazone, (B) SR1664, (C) glibenclamide and (D) glimepiride. Kinase reactions were subjected to Western blotting against phosphorylated PPAR γ at Ser-273, PPAR γ or CDK5 (A-D, upper panels). ADP content of the same kinase reactions was determined by a chemoluminescent assay (A-D, lower graphs). Data are represented as means \pm SEM (n = 4). IC₅₀ values were determined from the fitted concentration-response curves. NT, not treated.

3.4. SUs reduce PPAR γ Ser-273 phosphorylation in WAT of HFD mice

During diet-induced obesity, mice develop insulin resistance and exhibit increased PPAR γ Ser-273 phosphorylation in WAT [19]. In order to assess *in vivo* relevance of our findings, we investigated if SUs also block PPAR γ phosphorylation in WAT of HFD mice. After treatment for 6 days with a twice-daily i.p. dose of 10 mg/kg we determined mean plasma concentrations of 5 μ M, 7 μ M and 20 μ M for glimepiride, glibenclamide and rosiglitazone, respectively (Figure S2A). All

drugs caused a similar decrease in the phosphorylation of PPAR γ Ser-273 in WAT (Figure 4A) and an increase in GLUT4 protein expression as demonstrated by immunohistochemistry (Figure 4B). Although we did not observe a treatment-related reduction in crown-like structures in WAT stained with the macrophage marker F4/80 as signs of macrophage infiltration (Figure 4B), F4/80 mRNA expression was reduced by 24% for glimepiride (not significant) and about 50% for glibenclamide and rosiglitazone (Figure 4C). There was also increased expression of *aP2*, adiponectin and *Glut4* mRNA in WAT of all treatment groups albeit

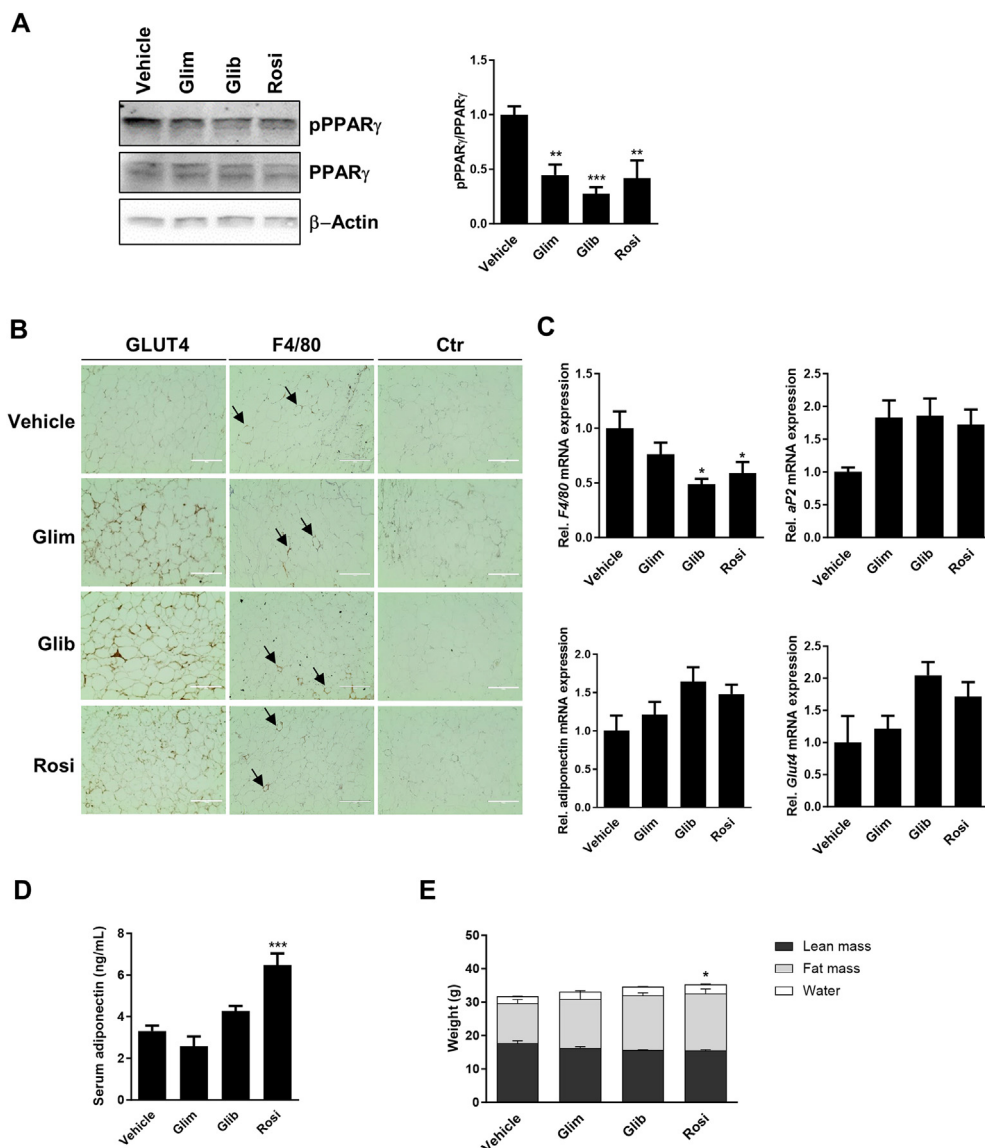


Figure 4: White adipose tissue (WAT) analysis of high-fat diet (HFD) mice after 6 days treatment with glimepiride (Glim), glibenclamide (Glib) and rosiglitazone (Ros). (A) Western blot against phosphorylated PPAR γ at Ser-273 (pPPAR γ). PPAR γ and β -Actin Western blots were performed to control for loading (left), quantification of relative PPAR γ phosphorylation vs. PPAR γ expression (right). (B) Immunohistochemistry of GLUT4 and F4/80 expression in WAT, crown-like structures are marked with an arrow. Control slides (Ctr) were stained with hematoxylin and secondary antibodies; scale bar 200 μ m. (C) Relative F4/80, aP2, adiponectin and Glut4 mRNA expression in WAT was determined by qRT-PCR. (D) Adiponectin serum levels and (E) body composition of HFD mice. Data are represented as means \pm SEM (n = 5). *, $p \leq 0.05$; **, $p \leq 0.01$; ***, $p \leq 0.001$ vs Vehicle, One-way ANOVA with Dunnett's post-hoc test.

this did not reach statistical significance (Figure 4C). In line with the increase in mRNA abundance, we measured slightly increased adiponectin serum levels in glibenclamide-treated mice. A statistical significant 2-fold increase was induced by rosiglitazone while glimepiride had no effect (Figure 4D). Only rosiglitazone induced minor changes in body composition (slightly increased fat and water mass; Figure 4E), but there were no effects on blood glucose, serum triglycerides and cholesterol levels by any of the drugs (Figure S2B–E). When we starved mice overnight, SU-treated mice exhibited a paradox increase in blood glucose and reduced glucose tolerance while rosiglitazone reduced blood glucose as expected (Figure S2B and F). This phenomenon might be the result of counterregulatory mechanisms after chronic SU treatment and overnight starving [35,36].

3.5. SUs alter adipocyte morphology and thermogenic marker expression in BAT of HFD mice

Glibenclamide and some PPAR γ Ser-273 blockers can induce thermogenic gene expression in BAT and impact brown adipocyte morphology [37–42]. Therefore, we also performed a histological analysis of BAT. As expected [43], H&E staining of BAT of rosiglitazone-treated mice was characterized by larger lipid droplets and significantly increased weight (+33%) as compared to BAT from control mice (Figure 5A–C). In contrast, SU treatment resulted in much smaller lipid droplets with no significant changes in BAT mass (Figure 5A–C). These changes were accompanied by increased UCP1 expression as determined by immunohistochemistry and qRT-PCR analyses. While visual changes in UCP1 protein expression were small in the

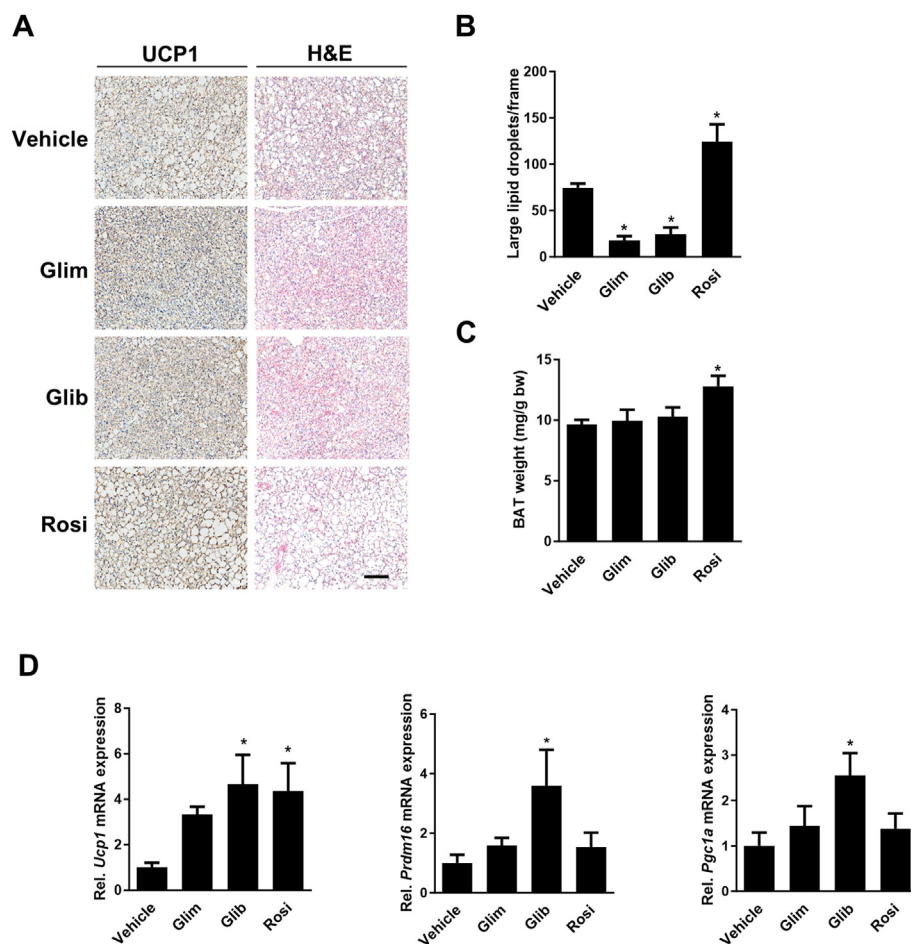


Figure 5: Brown adipose tissue (BAT) analysis of high-fat diet (HFD) mice after 6 days treatment with glimepiride (Glim), glibenclamide (Glib) and rosiglitazone (Rosi). (A) Hematoxylin/eosin (H&E) staining (right panels) and immunohistochemistry of UCP1 expression in BAT (left panels); scale bar 100 μm . (B) Quantification of lipid droplet sizes per 20x magnification frame/mouse. Large lipid droplets were defined as surface $>300 \mu\text{m}^2$. (C) BAT weight per g body weight (bw). (D) Relative *Ucp1*, *Prdm16* and *Pgc1a* mRNA expression was determined by qRT-PCR in BAT. Data are represented as means \pm SEM (n = 5). *, $p \leq 0.05$ vs Vehicle, One-way ANOVA with Dunnett's post-hoc test.

immunohistochemistry (Figure 5A), *Ucp1* mRNA increased by 3.3-, 4.7- and 4.4-fold after treatment with glimepiride, glibenclamide and rosiglitazone, respectively (Figure 5D). The mRNAs of two other thermogenic markers, PR domain containing 16 (*Prdm16*) and Peroxisome proliferator-activated receptor gamma coactivator 1 α (*Pgc1a*), were only significantly increased by glibenclamide.

3.6. *In silico* modelling of ligand binding to PPAR γ

To gain a structural knowledge of how SUs bind to PPAR γ in comparison to rosiglitazone and SR1664, we used an *in silico* modelling approach. We found eight different crystal structures of PPAR γ bound to rosiglitazone and two bound to SR1664 in the Protein Data Bank (PDB). Multiple structural alignments of those crystal structures showed that both ligands occupied similar positions. Rosiglitazone occupied the core of the PPAR γ LBD interacting with multiple residues on two helices surrounding this core region as well as on a β -stranded region that connects two helices and is surrounded on the periphery by a loop that bears the Ser-273 residue (Figure S3A). SR1664 also occupies a similar position but like rosiglitazone, it has no direct contacts with the Ser-273 residue. Instead, it interacts with the β -stranded region proximal to this critical residue (Figure S3B). Although the Ser-273 residue is located on a flexible region, it does not show any major shift (everything $<1 \text{ \AA}$) in backbone in the different conformers of all

these ligand bound complexes. The docking of rosiglitazone, SR1664 and both SUs onto a ligand-bound PPAR γ crystal structure (2hfp) [44] from which the ligand was manually removed, suggested the following binding characteristics: A) The top 5 docks for rosiglitazone (Figure 6A) and SR1664 (Figure 6B) were within 1 \AA of the region observed for these ligands in their crystal structures validating our docking results. B) The top 5 docks for rosiglitazone and glibenclamide (Figure 6A,C) all converged onto one particular ensemble which was within the core of the PPAR γ LBD. C) The top 5 docks for glimepiride (Figure 6D) on the other hand belong to three separate ensembles, all of which have mostly surface presence i.e. none of them are located deep in the core of the LBD. Only one of these ensembles (number 1 in Figure 6D) is partially embedded and more interestingly directly interacts with the loop region bearing the Ser-273 residue where it might interfere with Ser-273 phosphorylation. D) Three of 5 top docking ensembles of SR1664 were surface bound with one of them (number 4 in Figure 6B) close to the loop on which the Ser-273 residue resides. One of the ensembles corresponds to the original location of SR1664 observed in reported crystal structures i.e. the core of the PPAR γ LBD (number 3 in Figure 6B). Therefore, it seems that SR1664 shows binding modes that are similar to both glibenclamide/rosiglitazone and glimepiride. In a next step, we compared a native unbound PPAR γ structure generated by the I-TASSER threading server to the ligand-bound structures.

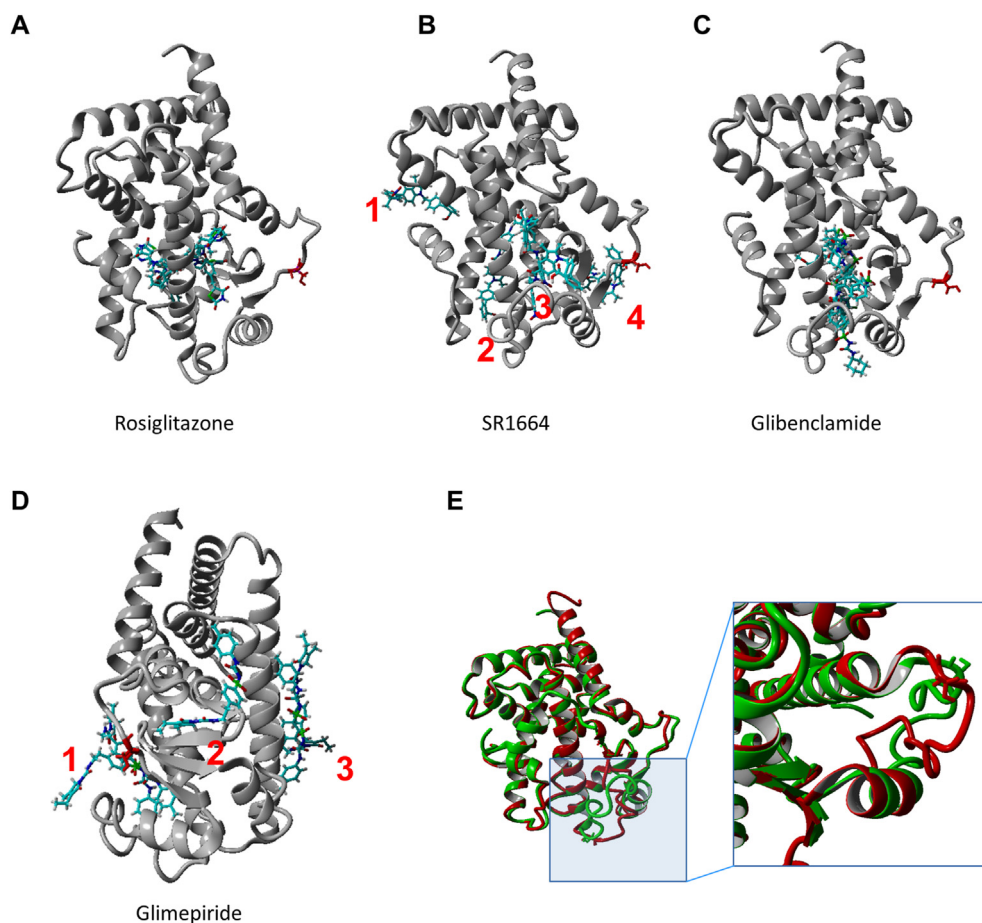


Figure 6: Docking of ligands onto PPAR γ structure and structural alignment of bound (2hfp) and unbound (model) ligand binding regions.

Top 5 docking poses for (A) rosiglitazone, (B) SR1664, (C) glibenclamide and (D) glimepiride. In each panel, the protein backbone is depicted in grey colored ribbon format with the ligand shown as stick models colored atom wise. The Ser-273 residue is depicted in each panel as a red colored stick model depiction. In case of docking poses belonging to different regions/ensembles they have been numbered. (E) Structural alignment bound (2hfp; green ribbon depiction) and unbound (model; red ribbon depiction) ligand binding regions. The inset image shows a closer view of the loop bearing the Ser-273 residue. The Ser-273 residue is depicted in stick model format.

However, using the complete PPAR γ protein yielded very poor scores (C score: 2–23, Figure S4). We observed that this was owed to lack of adequate threading templates for the DNA-binding region. The ligand-binding region within the model showed excellent alignment with various threaded templates and root mean squared deviation (RMSD) between 0.8 and 1.5 Å for the top ten templates. Therefore, for comparison we only considered the ligand-binding region i.e. between residues 230–515 from the model. When we aligned the model to the ligand-bound (i.e. rosiglitazone and SR1664) structures of PPAR γ we observed that almost the entire protein except for the loop region containing Ser-273 aligns perfectly. This loop region shows a drastic conformational change when compared to the same region within the unbound structure with an average RMSD of residues from this region >4 Å (Figure 6E), which could interfere with phosphorylation of the Ser-273 residue.

4. DISCUSSION

Transcriptional activation of PPAR γ in white adipocytes has been suggested as extra-pancreatic mechanism by which SUs increase insulin sensitivity and reduce cytokine expression a part from their

classical action on pancreatic β -cells [8–10,12,13,15]. However, it was questioned whether these effects on adipocytes are indeed mediated via classical transcriptional activation of PPAR γ or alternative mechanisms like interference with PPAR γ phosphorylation as described for several PPAR γ ligands [45]. Inhibition of PPAR γ Ser-273 phosphorylation by PPAR γ ligands requires binding to the LBD [19]. Although binding of SUs to the LBD has been proposed by several groups [8,12,13,15], it was unclear so far whether SUs also interfere with Ser-273 phosphorylation. Here, we show that glibenclamide and glimepiride exert similar effects on PPAR γ Ser-273 phosphorylation as the full PPAR γ agonist rosiglitazone and the PPAR γ ligand SR1664 in *in vitro* kinase assays. While glibenclamide was equally potent as rosiglitazone and SR1664 (IC₅₀s: 25 nM, 21 nM, and 17 nM, respectively), glimepiride had a 15-fold lower potency (IC₅₀: 378 nM) on phosphorylation inhibition. Our *in silico* PPAR γ binding analysis revealed that the mode of action of glibenclamide is quite similar to rosiglitazone. Both bind to the core of the protein (i.e. the LBD) inducing a conformational change that allosterically alters the protein surface (i.e. the Ser-273 residue). This mode of action was not observed for glimepiride as it does not bind to the LBD. On the other hand, glimepiride might directly interfere with the protein surface and the Ser-

273 residue, however, no docking pose was partially favoured in the docking analysis. Therefore, this binding is probably of low affinity which might account for its lower potency observed in kinase assays. In patients, the maximum plasma concentrations of glibenclamide and glimepiride are around 1 μM [46,47]. Thus, also clinical concentrations should cause an inhibition of PPAR γ Ser-273 phosphorylation in adipocytes. Applying glibenclamide and glimepiride at concentrations close to the clinical range (2.5 μM) was sufficient to suppress TNF- α -induced Ser-273 phosphorylation in primary human adipocytes. Consequently, we observed modulation of Ser-273-related genes such as up regulation of adiponectin and down regulation of pro-inflammatory cytokines similar to SR1664. However, in contrast to SUs and rosiglitazone, SR1664 did not suppress expression of *MCP1* and *IL6*. Similar findings have been reported for murine 3T3-L1 adipocytes [27]. Thus, glibenclamide and glimepiride mediate a distinct PPAR γ transcriptional activation, which is required to modulate expression of *MCP1* and *IL6*.

Short-term treatment of HFD mice reduced phosphorylation of PPAR γ Ser-273 in WAT by SUs comparable to rosiglitazone. However, we did not observe strong effects of the drugs on body composition, serum chemistry, adipogenic marker expression and adipose tissue inflammation in line with previous short-term studies performed with TZDs [19,20]. Nevertheless, rosiglitazone improved glucose tolerance. SUs induced a paradox effect, which was characterized by increased fasting plasma glucose levels and a negative impact on glucose tolerance. This phenomenon has previously been described after subacute and chronic SU-treatment of mice [35,36]. β -cell desensitization has been suggested as underlying mechanism resulting in an impairment of insulin secretion. In patients, these paradox effects are usually only observed after much longer treatment periods [35,36]. Therefore, longer treatment of mice with SUs was not considered in our study.

It has previously been shown that glimepiride can induce GLUT4 expression in WAT of *SUR1*-deficient HFD rats without elevating insulin, indicating that glimepiride acts via an extra-pancreatic mechanism [48]. In line with this, both SUs also increased GLUT4 protein levels in WAT of HFD mice. Furthermore, in our model of (TNF α -induced) insulin-resistant primary human white adipocytes SUs and SR1664 likewise increased *GLUT4* expression and glucose uptake. Thus, down-regulation of GLUT4 expression and reduced glucose uptake in white adipocytes during diabetic processes might be linked to PPAR γ Ser-273 phosphorylation and could be counteracted by SUs. Several PPAR γ Ser-273 blocker reduce adipogenesis in BAT and WAT while increasing thermogenic gene expression and energy expenditure [38–42]. This is in contrast to classical TZDs, which induce adipogenesis leading to weight gain despite increased energy expenditure. This is somehow surprising because the induction of a thermogenic gene program by PPAR γ ligands has been linked to full PPAR γ agonism [43]. One explanation might be that some PPAR γ ligands still have remaining PPAR γ transcriptional activity, which is sufficient to induce thermogenic gene expression. On the other hand, the NAD-dependent deacetylase SirT1 is able to deacetylate PPAR γ at Lys-268 and Lys-293 thereby driving TZD-induced browning of WAT [49,50]. Considering that the Ser-273 residue is in close proximity to Lys-268 and Lys-293, some PPAR γ ligands might also interfere with PPAR γ deacetylation to induce thermogenic genes. Recently, increased thermogenesis and UCP1 expression has also been reported after glibenclamide treatment of HFD mice [37]. Similarly, we observed an induction of UCP1 expression in BAT and a reduction in lipid droplet sizes after SU treatment indicative of increased thermogenesis resembling the typical phenotype reported for many PPAR γ Ser-273

blocker [37–42]. Although we noted adipogenic effects of SUs in white adipocytes, this did not translate into increased adipogenesis in BAT as observed for rosiglitazone. Therefore, we assume that the SU-induced BAT phenotype is not related to PPAR γ agonist activity but might rather depend on PPAR γ Ser-273 phosphorylation or alternative mechanisms like interference with PPAR γ deacetylation.

In summary, we found that both SUs are able to inhibit PPAR γ Ser-273 phosphorylation in primary human white adipocytes *in vitro* and in obese mice. Although we did not directly show that inhibition of PPAR γ phosphorylation is linked to the observed antidiabetic effects we provide indirect evidence. For instance, both SUs modulate expression of adipokines and increase GLUT4 expression and glucose uptake similar to SR1664, which exclusively acts by blocking PPAR γ Ser-273 phosphorylation. In addition, the observed BAT phenotype was similar to what is observed after treatment of obese mice with some PPAR γ Ser-273 blockers and different to rosiglitazone. Glibenclamide was more potent in terms of phosphorylation inhibition in kinase assays and we also observed a higher PPAR γ transcriptional and adipogenic activity as compared to glimepiride. In this context it is noteworthy that T2DM patients treated with glibenclamide are at a higher risk of cardiovascular adverse events and weight gain, common side effects also observed with TZDs [51]. This could be due to the observed PPAR γ agonist and resulting adipogenic activity despite the beneficial blocking of PPAR γ Ser-273 phosphorylation. In line with its rather weak adipogenic activity, glimepiride treatment is associated with fewer of these side effects. Furthermore, glimepiride increases insulin sensitivity and reduces pro-inflammatory cytokines in patients [51]. This might be a result of its interference with PPAR γ Ser-273 phosphorylation. Studies of the PPAR γ Ser-273 phosphorylation status in tissues of patients treated with SUs could give insight if relevant inhibition can indeed be achieved in humans at clinically relevant doses.

5. CONCLUSION

Our data presented here propose a novel mode of action of SUs on adipocytes, which could help to further explain the insulin-sensitizing and anti-inflammatory effects of SUs observed in the clinic. A portion of this action might be mediated via their interference with PPAR γ Ser-273 phosphorylation rather than via classical agonistic activity in adipocytes.

FUNDING

This work was supported by an intramural funding of the Federal Institute for Drugs and Medical Devices (to B.H.) and by Deutsche Forschungsgemeinschaft (DFG, German Research Foundation) 450149205-TRR333 (to A.P.). The funders had no role in study design, data collection and analysis, decision to publish, or preparation of the manuscript.

CREDIT AUTHORSHIP CONTRIBUTION STATEMENT

Bodo Haas: Conceptualization, Formal analysis, Investigation, Supervision, Visualization, Writing — original draft. **Moritz David Sebastian Hass:** Formal analysis, Investigation, Writing - Original Draft, Visualization. **Alexander Voltz:** Investigation, Visualization. **Matthias Vogel:** Investigation, Visualization. **Julia Walther:** Investigation, Visualization. **Arijit Biswas:** Formal analysis, Investigation, Visualization, Writing — original draft. **Daniela Hass:** Investigation, Visualization. **Alexander Pfeifer:** Supervision, Writing — review & editing.

ACKNOWLEDGEMENTS

Scientific advice from Niels Eckstein (R.I.P.) and Peter Mayer is highly appreciated. We are grateful for technical assistance from Constanze Weinreis, Patricia Zehner, Timo Reichmann and Johanna Renz. Bruce Spiegelman and Ronald Kahn are acknowledged for providing plasmids.

DECLARATION OF COMPETING INTEREST

Authors declare that there are no conflicts of interests.

DATA AVAILABILITY

Data will be made available on request.

APPENDIX A. SUPPLEMENTARY DATA

Supplementary data to this article can be found online at <https://doi.org/10.1016/j.molmet.2024.101956>.

REFERENCES

- [1] Sun H, Saeedi P, Karuranga S, Pinkepank M, Ogurtsova K, Duncan BB, et al. IDF Diabetes Atlas: global, regional and country-level diabetes prevalence estimates for 2021 and projections for 2045. *Diabetes Res Clin Pract* 2022;183:109119.
- [2] ElSayed NA, Aleppo G, Aroda VR, Bannuru RR, Brown FM, Bruemmer D, et al. 9. Pharmacologic approaches to glycemic treatment: standards of care in diabetes—2023. *Diabetes Care* 2022;46(Supplement_1):S140–57.
- [3] Dahlén AD, Dashi G, Maslov I, Attwood MM, Jonsson J, Trukhan V, et al. Trends in antidiabetic drug discovery: FDA approved drugs, new drugs in clinical trials and global sales. *Front Pharmacol* 2022;12.
- [4] Kramer W, Muller G, Geisen K. Characterization of the molecular mode of action of the sulfonylurea, glimepiride, at beta-cells. *Horm Metab Res* 1996;28(9):464–8.
- [5] Kabadi MU, Kabadi UM. Effects of glimepiride on insulin secretion and sensitivity in patients with recently diagnosed type 2 diabetes mellitus. *Clin Therapeut* 2004;26(1):63–9.
- [6] Koshiba K, Nomura M, Nakaya Y, Ito S. Efficacy of glimepiride on insulin resistance, adipocytokines, and atherosclerosis. *J Med Invest* 2006;53(1–2): 87–94.
- [7] Mori RC, Hirabara SM, Hirata AE, Okamoto MM, Machado UF. Glimepiride as insulin sensitizer: increased liver and muscle responses to insulin. *Diabetes Obes Metabol* 2008;10(7):596–600.
- [8] Fukuen S, Iwaki M, Yasui A, Makishima M, Matsuda M, Shimomura I. Sulfonylurea agents exhibit peroxisome proliferator-activated receptor gamma agonistic activity. *J Biol Chem* 2005;280(25):23653–9.
- [9] Inukai K, Watanabe M, Nakashima Y, Takata N, Ioyama A, Sawa T, et al. Glimepiride enhances intrinsic peroxisome proliferator-activated receptor-gamma activity in 3T3-L1 adipocytes. *Biochem Biophys Res Commun* 2005;328(2):484–90.
- [10] Mayer P, Haas B, Celner J, Enzmann H, Pfeifer A. Glitazone-like action of glimepiride and glibenclamide in primary human adipocytes. *Diabetes Obes Metabol* 2011;13(9):791–9.
- [11] Muller G, Geisen K. Characterization of the molecular mode of action of the sulfonylurea, glimepiride, at adipocytes. *Horm Metab Res* 1996;28(9):469–87.
- [12] Scarsi M, Podvenc M, Roth A, Hug H, Kersten S, Albrecht H, et al. Sulfonylureas and glinides exhibit peroxisome proliferator-activated receptor gamma activity: a combined virtual screening and biological assay approach. *Mol Pharmacol* 2007;71(2):398–406.
- [13] Lee KW, Ku YH, Kim M, Ahn BY, Chung SS, Park KS. Effects of sulfonylureas on peroxisome proliferator-activated receptor gamma activity and on glucose uptake by thiazolidinediones. *Diabetes Metab J* 2011;35(4):340–7.
- [14] Tontonoz P, Spiegelman BM. Fat and beyond: the diverse biology of PPAR-gamma. *Annu Rev Biochem* 2008;77:289–312.
- [15] Arrault A, Rocchi S, Picard F, Maurois P, Pirotte B, Vamecq J. A short series of antidiabetic sulfonylureas exhibit multiple ligand PPARgamma-binding patterns. *Biomed Pharmacother* 2009;63(1):56–62.
- [16] Forman BM, Tontonoz P, Chen J, Brun RP, Spiegelman BM, Evans RM. 15-Deoxy-delta 12, 14-prostaglandin J2 is a ligand for the adipocyte determination factor PPAR gamma. *Cell* 1995;83(5):803–12.
- [17] Lehmann JM, Moore LB, Smith-Oliver TA, Wilkison WO, Willson TM, Kliewer SA. An antidiabetic thiazolidinedione is a high affinity ligand for peroxisome proliferator-activated receptor gamma (PPAR gamma). *J Biol Chem* 1995;270(22):12953–6.
- [18] Mastrototaro L, Roden M. Insulin resistance and insulin sensitizing agents. *Metabolism* 2021;125:154892.
- [19] Choi JH, Banks AS, Estall JL, Kajimura S, Bostrom P, Laznik D, et al. Anti-diabetic drugs inhibit obesity-linked phosphorylation of PPARgamma by Cdk5. *Nature* 2010;466(7305):451–6.
- [20] Choi JH, Banks AS, Kamenecka TM, Busby SA, Chalmers MJ, Kumar N, et al. Antidiabetic actions of a non-agonist PPARgamma ligand blocking Cdk5-mediated phosphorylation. *Nature* 2011;477(7365):477–81.
- [21] Banks AS, McAllister FE, Camporez JP, Zushin PJ, Jurczak MJ, Laznik-Bogoslavski D, et al. An ERK/Cdk5 axis controls the diabetogenic actions of PPARgamma. *Nature* 2015;517(7534):391–5.
- [22] Choi JH, Choi SS, Kim ES, Jedrychowski MP, Yang YR, Jang HJ, et al. Thrap3 docks on phosphoserine 273 of PPARgamma and controls diabetic gene programming. *Genes Dev* 2014;28(21):2361–9.
- [23] Dias MMG, Batista FAH, Tittanegro TH, de Oliveira AG, Le Maire A, Torres FR, et al. PPARgamma S273 phosphorylation modifies the dynamics of coregulator proteins recruitment. *Front Endocrinol* 2020;11:561256.
- [24] Hall JA, Ramachandran D, Roh HC, DiSpirito JR, Belchior T, Zushin PH, et al. Obesity-linked PPARgamma S273 phosphorylation promotes insulin resistance through growth differentiation factor 3. *Cell Metabol* 2020;32(4):665–675 e666.
- [25] Khim KW, Choi SS, Jang HJ, Lee YH, Lee E, Hyun JM, et al. PPM1A controls diabetic gene programming through directly dephosphorylating PPARgamma at Ser273. *Cells* 2020;9(2).
- [26] Acton III JJ, Black RM, Jones AB, Moller DE, Colwell L, Doebber TW, et al. Benzoyl 2-methyl indoles as selective PPARgamma modulators. *Bioorg Med Chem Lett* 2005;15(2):357–62.
- [27] Choi SS, Kim ES, Koh M, Lee SJ, Lim D, Yang YR, et al. A novel non-agonist peroxisome proliferator-activated receptor gamma (PPARgamma) ligand UHC1 blocks PPARgamma phosphorylation by cyclin-dependent kinase 5 (CDK5) and improves insulin sensitivity. *J Biol Chem* 2014;289(38):26618–29.
- [28] Niemann B, Haufs-Brusberg S, Puetz L, Feickert M, Jaeckstein MY, Hoffmann A, et al. Apoptotic brown adipocytes enhance energy expenditure via extracellular inosine. *Nature* 2022;609(7926):361–8.
- [29] Mitschke MM, Hoffmann LS, Gnad T, Scholz D, Kruihthoff K, Mayer P, et al. Increased cGMP promotes healthy expansion and browning of white adipose tissue. *Faseb J* 2013;27(4):1621–30.
- [30] Haas B, Mayer P, Jennissen K, Scholz D, Berriel Diaz M, Bloch W, et al. Protein kinase G controls brown fat cell differentiation and mitochondrial biogenesis. *Sci Signal* 2009;2(99):ra78.
- [31] Chen Y, Siegel F, Kipschull S, Haas B, Frohlich H, Meister G, et al. miR-155 regulates differentiation of brown and beige adipocytes via a bistable circuit. *Nat Commun* 2013;4:1769.

- [32] Kim JB, Wright HM, Wright M, Spiegelman BM. ADD1/SREBP1 activates PPARgamma through the production of endogenous ligand. *Proc Natl Acad Sci U S A* 1998;95(8):4333–7.
- [33] Tontonoz P, Hu E, Graves RA, Budavari AI, Spiegelman BM. mPPAR gamma 2: tissue-specific regulator of an adipocyte enhancer. *Genes Dev* 1994;8(10):1224–34.
- [34] Gilani A, Stoll L, Homan EA, Lo JC. Adipose signals regulating distal organ health and disease. *Diabetes* 2024;73(2):169–77.
- [35] Niedowicz DM, Ozcan S, Nelson PT. Glimepiride administered in chow reversibly impairs glucose tolerance in mice. *J Diabetes Res* 2018;2018:1251345.
- [36] Remedi MS, Nichols CG. Chronic antidiabetic sulfonylureas in vivo: reversible effects on mouse pancreatic beta-cells. *PLoS Med* 2008;5(10):e206.
- [37] Qiu Y, Yang Y, Wei Y, Liu X, Feng Z, Zeng X, et al. Glyburide regulates UCP1 expression in adipocytes independent of K(ATP) channel blockade. *iScience* 2020;23(9):101446.
- [38] Terra MF, Garcia-Arevalo M, Avelino TM, Degaki KY, Malospirito CC, de Carvalho M, et al. AM-879, a PPARγ non-agonist and Ser273 phosphorylation blocker, promotes insulin sensitivity without adverse effects in mice. *Metabol Open* 2023;17:100221.
- [39] Coelho MS, de Lima CL, Royer C, Silva JB, Oliveira FC, Christ CG, et al. GQ-16, a TZD-derived partial PPARgamma agonist, induces the expression of thermogenesis-related genes in Brown fat and visceral white fat and decreases visceral adiposity in obese and hyperglycemic mice. *PLoS One* 2016;11(5):e0154310.
- [40] Huan Y, Pan X, Peng J, Jia C, Sun S, Bai G, et al. A novel specific peroxisome proliferator-activated receptor gamma (PPARgamma) modulator YR4-42 ameliorates hyperglycaemia and dyslipidaemia and hepatic steatosis in diet-induced obese mice. *Diabetes Obes Metabol* 2019;21(11):2553–63.
- [41] Yu J, Hu Y, Sheng M, Gao M, Guo W, Zhang Z, et al. Selective PPARgamma modulator diosmin improves insulin sensitivity and promotes browning of white fat. *J Biol Chem* 2023;299(4):103059.
- [42] Wu D, Eeda V, Undi RB, Mann S, Stout M, Lim HY, et al. A novel peroxisome proliferator-activated receptor gamma ligand improves insulin sensitivity and promotes browning of white adipose tissue in obese mice. *Mol Metabol* 2021;54:101363.
- [43] Ohno H, Shinoda K, Spiegelman BM, Kajimura S. PPARgamma agonists induce a white-to-brown fat conversion through stabilization of PRDM16 protein. *Cell Metabol* 2012;15(3):395–404.
- [44] Hopkins CR, O'Neil S V, Laufersweiler MC, Wang Y, Pokross M, Meikel M, et al. Design and synthesis of novel N-sulfonyl-2-indole carboxamides as potent PPAR-gamma binding agents with potential application to the treatment of osteoporosis. *Bioorg Med Chem Lett* 2006;16(21):5659–63.
- [45] Frkic RL, Richter K, Bruning JB. The therapeutic potential of inhibiting PPARgamma phosphorylation to treat type 2 diabetes. *J Biol Chem* 2021;297(3):101030.
- [46] Langtry HD, Balfour JA. Glimepiride. A review of its use in the management of type 2 diabetes mellitus. *Drugs* 1998;55(4):563–84.
- [47] Coppack SW, Lant AF, McIntosh CS, Rodgers AV. Pharmacokinetic and pharmacodynamic studies of glibenclamide in non-insulin dependent diabetes mellitus. *Br J Clin Pharmacol* 1990;29(6):673–84.
- [48] Zhou X, Zhang R, Zou Z, Shen X, Xie T, Xu C, et al. Hypoglycaemic effects of glimepiride in sulfonylurea receptor 1 deficient rat. *Br J Pharmacol* 2019;176(3):478–90.
- [49] Qiang L, Wang L, Kon N, Zhao W, Lee S, Zhang Y, et al. Brown remodeling of white adipose tissue by SirT1-dependent deacetylation of Ppargamma. *Cell* 2012;150(3):620–32.
- [50] Kraakman MJ, Liu Q, Postigo-Fernandez J, Ji R, Kon N, Larrea D, et al. PPARgamma deacetylation dissociates thiazolidinedione's metabolic benefits from its adverse effects. *J Clin Invest* 2018;128(6):2600–12.
- [51] Kalra S, Das AK, Baruah MP, Unnikrishnan AG, Dasgupta A, Shah P, et al. Glucocronology of modern sulfonylureas: clinical evidence and practice-based opinion from an international expert group. *Diabetes Ther* 2019;10(5):1577–93.